# Fixed-bed Adsorption of Congo red dye and Bisphenol A from solution onto surfactant modified walnut shell

**Evans Dovi**
Zhengzhou University
**Aaron Albert Aryee**
Zhengzhou University
**Alexander Nti Kani**
Zhengzhou University
**Farid Mzee Mpatani**
Zhengzhou University
**Jianjun Li**
Zhengzhou University
**Zhaohui Li**
Zhengzhou University
**Lingbo Qu**
Zhengzhou University
**Runping Han** ( rphan67@zzu.edu.cn )
Zhengzhou University https://orcid.org/0000-0002-1585-4522

**Research Article**

**Keywords:** Modified walnut shell, Congo red, Bisphenol A, Column adsorption, Regeneration

**Posted Date:** March 2nd, 2021

**DOI:** https://doi.org/10.21203/rs.3.rs-243098/v1

**Fixed-bed Adsorption of Congo red dye and Bisphenol A from solution onto surfactant modified walnut shell**

Evans Dovi [1], Aaron Albert Aryee [1], Alexander Nti Kani [1], Farid Mzee Mpatani [1], Jianjun Li [1], Zhaohui Li[*1], Lingbo Qu [1], Runping Han[*1]

[1]College of Chemistry, Green Catalysis Center, Zhengzhou University, No 100 of Kexue Road, Zhengzhou, 450001 P. R. China

[*] Corresponding authors. E-mail address: zhaohui.li@zzu.edu.cn (Z. Li), rphan67@zzu.edu.cn (R. Han)

**Abstract**

Wastewater stemming from industries may contain pollutants such as synthetic dyes and endocrine-disrupting chemicals which are known to be harmful to living organisms. Therefore, to safeguard the wellbeing of humankind and environmental safety, it is imperative for industrial effluents to be sanitized before their discharged into water bodies. Furthermore, to explore the utilization of agricultural byproduct is valuable to study. To achieve this, a Cetyltrimethylammonium bromide functionalized Walnut shells (WNS-CTAB) were prepared to remove pollutants in column approach. The column work was carried out for diverse working conditions. There is in favor of adsorption at low influent pollutant concentration, low flow rate or high bed depth. As the highest breakthrough time of 113 and 23 min at flow rate 6 mL $min^{-1}$ was recorded for both CR and BPA, respectively, the Yan's kinetic model best described the breakthrough curve. The adsorbent showed better regeneration capabilities; accordingly can offer practical use for adsorption of CR and BPA from wastewaters.

**Keywords**: Modified walnut shell; Congo red; Bisphenol A; Column adsorption; Regeneration

## 1. Introduction

The existence of living organisms largely depends on water; therefore, it is imperative to ensure that the quality and safety of water is guaranteed. However, activities undertaken by humankind tend to overlook the quality of our aquatic bodies The textile, leather, paper, printing industries that employ the use of dyes in their operation tend to pollute water bodies by disposing into them large amount of wastewater containing dyes residues (Bhaumik et al., 2013;Hou et al. 2012) Dye-containing wastewater is harmful and coloured contaminant that causes grave health problems when disposed into aquatic system prior to its purification (Kumar et al., 2010; Bhaumik et al., 2013). Congo red (CR) has been known to possess carcinogenic and mutagenic effects (Mane and Vijay Babu, 2013)

On the other hand, the occurrence of emerging micro-pollutant (EMPs) has been observed to be on the increased in water bodies, which are identified to be injurious to life in the ecological unit (Mpatani et al., 2020a). EMPs normally exist in their free state or in combination with organic compounds like pesticides and food additives (Paterni et al.,2018). Among these anthropogenic substances is BPA which is identified as endocrine-disrupting chemicals (EDCs).which is largely employed as a precursor for the manufacturing of plastics (Zhou et al., 2012).

Widespread usage of CR and BPA in both domestic and industrial products has contributed to its discharge to the environment. Whiles the presence of CR molecules, an important class of recalcitrant organic compound, in the wastewater are aesthetically displeasing and undesirable (Kani et al., 2021) owing to their and mutagenic and carcinogenic effects to both water fauna and human beings (Kani et al., 2020), BPA on the other hand is a xenoestrogen, which is an estrogen-imitating compound which could negatively influence the health of humankind (Zhou et al., 2012). These compounds (CR and BPA) have been reported to have high molecular stability, poor biodegradation and resilient to biochemical breakdown (Mpatani et al., 2020 a; Kani et al., 2020). The existence of these contaminants raises significant environmental apprehensions that require to be dealt with. Hence, the need to devise a practicable approach which could uptake BPA and dyes from wastewater before it is released into the water body to preserve the quality and avoid the scarcity of water.

Several physicochemical techniques have been formulated for removal of pollutants before their release into the aquatic systems. Techniques such as adsorption, flotation, chemical precipitation, reverse osmosis. Among these techniques, adsorption has been acknowledged to be valuable and proficient process for purification of water due to its straightforwardness, inexpensive, eco-friendly, and effectiveness (Kani et al., 2020; Aryee et al., 2021).

Commercial activated carbon is very proficient material for the uptake of contaminants (Chang et al., 2012). However, it is very expensive and hard to regenerate makes its utilization in the purification of water very restricted (Shang et al., 2015). Thus, the need to develop cheap, practical and effective adsorbents is exigent for the uptake of pollutants. Recently, utilization of agricultural wastes (AW) as adsorbent for adsorption of pollutants has received massive attention owing to their accessibility and being economical (Aryee et al., 2020a; Cao et al., 2014; Kani et al., 2020; Zhang et al., 2012). Several AW like corn cob, rice husk, tea waste and mango seed have been used to remove pollutants from solutions because of their accessibility and eco-friendliness. Majority of AW seemed to possess low adsorption ability when used in raw state. As a result this, AW are chemically modified to overcome the problem of low removal (Xu et al., 2016; Aryee et al., 2020 b; Zhang et al., 2014). A typical example is the alteration of WNS with amine groups that enhanced metal ions removal substantially owing to the bonding

capability, formation of complex or ionic interaction between the functionalized adsorbent and metal ions (Cao et al., 2014).

Walnut (*Juglans regia L.*) is produced mainly as food. World production of walnuts is more than 2 million metric tons, China being the major producer. Owing to the widely consumption walnut, large quantity of wastes are likely to be produced. These wastes are either burned or buried. The buried wastes do not decay readily because of its hardness and hence remain in the soil for a very longtime causing nuisance to the environment. (Zhao et al, 2020). Nevertheless, large amount of carbon (IV) oxide could emanate from the burning of walnut wastes which is a potential pollutant and might contribute to global warming. Research revealed that walnut shell possesses outstanding properties such as large surface area, good stability and good chemical stability, thus could be an important precursor for use in the industry (Cao et al., 2014; Li et al., 2020; Dovi et al., 2021). Hence, using walnut shells which is copiously available, cheap, and easiness to work with, in the area of adsorption to remove waste water could be well thought-out to be safe and eco- friendly.

Herein, an apt, environmental-friendly and cheap adsorbent, WNS-CTAB (cetyltrimethylammonium bromide modified walnut shell), has been developed for BPA and CR removal from aqueous solutions by adsorption procedure in batch mode (Dovi et al., 2021). From this study, the modifying agents can improve the uptake capacity of WNS towards CR and BPA adsorption from aqueous solutions. However, several studies reported the use of adsorbents in the batch experimental mode for adsorption of pollutants but in industries, adsorptions in a packed columns are more desirable, and the outcome from the laboratory scale columns could be useful to apply in the industry (Baral et al., 2009; Calero et al., 2009). In this work, the use of WNS-CTAB was applied for adsorption Congo red and Bisphenol A from solution in column systems. The column performance and behavior of the breakthrough as a function of concentration, bed height and flow rate were studied. The breakthrough curves were described by Thomas, Clark and Yan models. Adsorption-desorption cycles were performed to find out adsorbent's reusability potentials. The process including was green and sustainable due to effective application of waste materials and removal of pollutants.

## 2. Materials and methods

### 2.1 Materials

Walnut shells (WNS) were collected from a market near Zhengzhou University. Congo red (CR, $C_{32}H_{22}N_6Na_2O_6S_2$), cetyltrimethylammonium bromide (CTAB), methanol ($CH_3OH$), absolute ethanol ($C_2H_5OH$), Bisphenol A (BPA) were acquired from Tian in Fuyu Fine Chemical Co., Ltd. sodium hydroxide (NaOH) and Hydrochloric acid (HCl) were procured from Zhengzhou Chemical Corporation, China. Analytical grade of reagents and solvents were used.

### 2.2. Preparation of CTAB modified walnut shell (WNS-CTAB)

The modification process was according to previous work (Dovi et al., 2021). Simply, the clean walnut shell was grinded and sieved to obtain particle with 40-60 mesh. One gram of WNS and 20 mL NaOH (0.4 mol $L^{-1}$) solution were placed in flask and stirred continuously for 6 h. The WNS was taken from solution and washed several times to neutral and dried at 60 $^oC$ for 12 h. Then the pretreated WNS was placed in 100 mL of 1% CTAB solution

and was agitated at 303 K for 24 h. Next, the material was taken out solution and rinsed with ultrapure water several times, dried at 60 °C for 12 h and WNS-CTAB was obtained.

WNS-CTAB was characterized using XPS and FTIR and the results showed that there was successful modification. The uneven and the pores of WNS-CTAB may be in favor of the uptake of BPA and CR.

**2.3. Preparation of BPA and CR solution**

A 1000 mg $L^{-1}$ solution of CR and Bisphenol A were made by separately dissolving 1000 mg of pollutants solutes in 1000 mL of distilled water forming the stock solution of each pollutant. Working solution was made by diluting the stock solution to the required concentrations.

**2.4. Column adsorption studies**

Column uptake experiment was executed at 303K and pH 6 using WNS-CTAB loaded into a glass tube (inner diameter of 1.3 cm and a length 30 cm) with a bed height of 3 cm (1.64 g), 6 cm (3.25 g), and 9 cm (4.89 g). Attached to the bottom of column was a stainless sieve with a layer of cotton wool to support and avert adsorbent lost. The experiments were performed by pumping CR and BPA solution into the column in downward flowing mode with a peristaltic pump and the effluent were taken at regular interval in the removal process. UV spectrophotometer (Persee TU-1800, China) was employed to measure the concentration of the effluent at 497 nm for CR and 276 nm for BPA as maximum adsorption wavelength.

**2.5. Column data analysis**

The nature of breakthrough graphs are vital charateristics for establishing the operation and continuous reaction of column adsorption (Ahmad and Hameed 2010; Han et al., 2009). The point at which the concentration of pollutants ($C_t$) emanating from the column gets to almost 0.01% of the starting solution is known as the breakthrough point while the column exhaustion point is usually the point where the concentration of effluent is almost the same as the starting solution (Kundu et al., 2004). Generally, breakthrough performance is achieved by plotting $C_t/C_0$ versus time, $t$ (Han et al., 2009; Kundu et al., 2004). The volume of effluent, $V_{eff}$ (mL), can be estimated by Eq. 1 (Chen et al., 2012).

$$V_{eff} = vt_{total} \quad (1)$$

Where $v$ is the flowing rate (mL $min^{-1}$), $t_{total}$ is the total flowing time (min). The value of the total mass of pollutants adsorbed, $q_{total}$ (mg), can be estimated from the area beneath the breakthrough curve (Eq. 2) (Han et al., 2009).

$$q_{total} = \frac{v}{1000}\int_{t=0}^{t=t_{total}} (C_0 - C_t)dt \quad (2)$$

where $C_0$ is the concentration of pollutants (mg $L^{-1}$), $x$ is the weight of dry adsorbent in the column (g), maximum column capacity, $q_{exp}$ (mg $g^{-1}$) is estimated with Eq. 3.

$$q_{exp} = q_{total} / x \quad (3)$$

**3. Results and Discussions**

**3.1 Column performance at varied operating conditions**

**3.1.1 Comparing breakthrough curves of WNS and WNS-CTAB**

Breakthrough curves of WNS and WNS-CTAB for the adsorption of CR and BPA are illustrated in Fig. 1(a) and (b), respectively. As exhibited in Fig. 1, the breakthrough time at $C_t/C_0 = 0.5$ for WNS and WNS-CTAB uptake of CR was 26 and 89 min, while that for BPA was 7 and 20 min respectively. Again, the breakthrough curves

presented by WNS for the adsorption of CR and BPA were very steep indicating poor removal of the pollutants. These outcomes affirm that the removal efficiency of WNS was enhanced greatly after its modification. The enhanced removal was due to the adsorbed cationic surfactant onto the surface of WNS. The surface of the modified adsorbent became cationic and non-polar, that made it more appropriate for the uptake of negatively charged CR dyes and BPA. The surface functional groups that promoted the uptake of CR and BPA were confirmed by FTIR and XPS analysis, respectively (Dovi et al., 2021). During the adsorption, the main interactive forces could be electrostatic attraction which may occur between the negative group of CR and $BPA^-$ molecules and cationic adsorbent and hydrophobic reaction between the phenyl group of the pollutants and the alkyl chain on the modified adsorbent (WNS-CTAB) is another interaction for the removal process (Xia et al., 2011).

**3.2. Influence of flow rate on breakthrough curves**

This work was conducted at various flowing rates (6, 10 and 14 mL $min^{-1}$) at the same height of column 6 cm and influent solution of 50 mg $L^{-1}$ for both CR and BPA. The curve illustrating the breakthrough for the column was established by plotting $C_t/C_0$ against time, $t$ as presented in Fig. 2 (a) and (b) for CR and BPA respectively. When the flowing rate was raised from 6 to14 mL $min^{-1}$, it led to reduction of time, pollutants stay in the column and appearance of early breakthrough. From Fig. 2, the breakthrough time at $C_t/C_0 = 0.5$ was found to be 113, 89 and 43 min and 23, 20 and 13 min at flow rates 6, 10, and 14 mL $min^{-1}$ for CR and BPA respectively. As the flowing rates were increased, the external film mass resistance at the adsorbent's surface reduced and the dwelling time also decreased, hence, decreasing the time of saturation, depicting poor uptake efficiency and lower breakthrough time (Han et al., 2009). Furthermore, less residence time turns to decrease the binding ability of the pollutants to the surface of the adsorbent, further resulting in a quicker breakthrough (Chen et al., 2012). Similar trends have been detailed by researchers like Aguayo-villarreal et al. (2011) and Vinodhini and Das (2010). The values of $q_{total}$ and $q_{exp}$ at varied experimental conditions are detailed in Table 1a.

**3.3. Influence of influent concentration on breakthrough curve**

This was investigated at varied concentrations of CR (30, 50 and 80 mg $L^{-1}$) and BPA (30, 50 and 70 mg $L^{-1}$) at the same height of column 6 cm and flowing rate 10 mL $min^{-1}$. From the breakthrough curve presented in Fig. 3, the removal phenomenon attained saturation faster and a shorten breakthrough time as concentrations increases. The breakthrough time at $C_t/C_0 = 0.5$ was determined as 143, 89 and 50 min at 30, 50, and 80 mg $L^{-1}$ for CR and 27, 20 and 15 min at 30, 50, and 70 mg $L^{-1}$ for BPA respectively. This phenomenon might be assigned to an increased in driving force for the removal of pollutants. However, an extension in breakthrough point was noticed at lesser concentrations of CR and BPA which was credited to lesser mass transfer in the removal process leading to more volume of CR and BPA being treated (Auta and Hameed, 2014). Han et al. (2009) also observed similar occurrence. The $q_{total}$ and $q_e$ values increased with an increased in the influent CR and BPA solution from 30 to 80 mg $L^{-1}$ and 30 to 70 mg $L^{-1}$, respectively, as shown in Table 1a. These results may be ascribed to the difference in column resistance and removal driving forces (Olgun et al., 2013).

**3.4. Influence of varied column heights on breakthrough curve**

The influence of various bed heights on breakthrough curve was operated at same initial solution of 50 mg $L^{-1}$ and flowing time of 10 mL $min^{-1}$ for both CR and BPA adsorption. Fig. 4 illustrates breakthrough curves at varied

column heights. The gradient of the curves reduced at enhanced column height, which culminated in an enlarged mass transfer zone (Olgun et al., 2013). The results illustrated that the time of saturation and breakthrough point increased when bed height or depth was increased from 3 to 9 cm. At $C_t/C_0$ = 0.5 the breakthrough time was found to be 48, 89 and 130 min for CR and 14, 20 and 27 min for BPA at bed depth 3, 6, and 9 cm respectively. An increased in the breakthrough time could be credited to an increased in adsorbent's surface area, enough bonding sites and adequate dwelling time of pollutants in the column's removal zone which allowed enough reaction time of the pollutants with the adsorbent. Similar observation was reported by Banerjee et al. (2018).

**3.5. Column data modeling**

**3.5.1. Thomas model application**

This model is usually employed to predict the performance theory of removal phenomenon in column and is given as (Aksu & Gonen, 2004) follows:

$$\frac{C_t}{C_0} = \frac{1}{1+\exp(k_{Th}q_0 x/v - k_{Th}C_0 t)} \quad (4)$$

where $C_t$ and $C_o$ are the effluent and influent pollutants concentration (mg $L^{-1}$), $k_{Th}$ is the Thomas rate constant (mL $min^{-1}$ $mg^{-1}$), $q_o$ is the maximum uptake quantity (mg $g^{-1}$), $x$ is the weight of material in the column (g), $V_{eff}$ ($vt$) is the effluent volume (mL) and $v$ is the flowing time (mL $min^{-1}$).

The column constant $k_{Th}$ and the uptake quantity of the column $q_o$ were decided by plotting $C_t/C_0$ versus $t$ at a particular condition and were analyzed by nonlinear regression and the outcomes are presented in Table 1b for CR and BPA, respectively. Fig. 2, 3 and 4 illustrate curves fitted with the Thomas model. From Table 1b, the $k_{Th}$ values increased as the solution's flow rate increases, however, the value of $k_{Th}$ reduced when the concentration of the pollutants increased. Again, the uptake capacity $q_o$ was enhanced with an increased in influent concentration and reduces with an increased in the bed height. This denotes that diffusion does not restrict the removal process was not restricted by diffusion (Baral et al., 2009; Han et al., 2009; Chen et al., 2012). As presented in Table 1b , the values of $q_{exp}$ were close to $q_o$ at the same condition for CR and BPA whereas the $R^2$ values were not higher than 0.993 and SSE ranging from 0.008 to 0.117. Moreover, the fitted curve was near at the initial parts but far away at the final sections of the experimental curves (Fig. 2, 3 and 4), hence the column performance could not be better described by Thomas model.

**3.6.2. Application of Clark model**

Clark model employs the mass-transfer concept together with the Freundlich isotherm (Clark 1987). The expression is given as:

$$\frac{C_t}{C_0} = \left(\frac{1}{1+Ae^{-rt}}\right)^{1/(n-1)} \quad (5)$$

where $A$ and $r$ are the Clark constants; $n$ is from Freundlich model. The Clark constants were determined by plotting $C_t/C_0$ versus $t$ at a given condition was analyzed by nonlinear regression. Values of $n$ were 3.52 for CR and 3.26 for BPA according to previous study in batch mode, respectively (Dovi et al., 2021). Fig. 2, 3 and 4 also show the fitted curves with the Clark model and Table 2 illustrates the parameters derived from nonlinear regressive analysis.

Based on the outcomes from the analysis exhibited in Table 2, the $r$ values improved with increasing both concentration and flowing rate for CR and BPA. Conversely, the values of $r$ decreased for both pollutants as the amount of adsorbents in the column increases. The fitted curves were very far from the experimental data as shown in Fig. 2, 3 and 4 at all the operating conditions for CR and BPA. This clearly shows that the breakthrough curves simulated by Clark were not able to predict the experimental curves better as compared to that of Yan. Furthermore, the $R^2$ and SSE values as presented in Table 2 and 3 confirmed Clark model could not described the breakthrough curves.

**3.6.3. Application of Yan model**

The Yan model is employed to ease the inaccuracies ensuing from the Thomas model, principally at early or final sections of the breakthrough curve. The eqn. is given as:

$$\frac{C_t}{C_0} = 1 - \frac{1}{1 + (vt/b)^a} \quad (6)$$

$$q_0 = \frac{bc_0}{x} \quad (7)$$

where $C_t$ and $C_0$ are the effluent and influent pollutants concentration (mg $L^{-1}$), $b$ and $a$ the Yan's constants. The Yan model (Yan et al., 2001) also provides for the adsorption quantity ($q_0$) which is calculated from Eq. (7).

The fitted curves from Yan model are also presented in Fig. 2, 3 and 4 and the parameters are listed in Table 4. The fitted curve was very near to the experimental curve as given in Fig. 2, 3 and 4 at all the operating conditions for CR and BPA. As provided in Table 3, $b$ increases as bed height increases but reduced while the rate of flow and concentration of the pollutants (CR and BPA) increases. Again, there were larger $R^2$ values and smaller values of SSE compared to the $R^2$ and SSE values from Thomas and Clark models at same conditions (as shown in Tables 1b, 2 and 3). This denoted that Yan model described the column uptake process better than both Thomas and Clark models. Similar outcome was reported by Zhou et al. (2015).

**3.7. Column reusability**

The capability of a spent adsorbent to be reused is of immense achievement as it advances its cost-effectiveness (Han et al., 2010; Mpatani et al., 2020b; Zhou et al., 2015). To renew the spent adsorbent, desorption was performed with 0.1 M NaOH and 75% ethanol for CR and BPA respectively. Two adsorption-desorption cycles were conducted in a continuous method and their breakthrough curves are presented in Fig. 5 a and b for CR, Fig. 5 c and d for BPA respectively.

The breakthrough time and pollutants removal ability for the two cycles are presented in Table 4. A reduced $t_b$, $q_e$ and $\%R$ were observed as the regeneration cycles advanced. This performance is chiefly as results of the steady declined of adsorbent because of its being used successively. It was also observed that the desorption efficiency was fairly constant in all the rounds of desorption. The outcome reveals that the adsorbent (WNS-CTAB) could still be employed for the uptake of pollutants in solution even after two cycles.

**4. Conclusion**

This work recognized modified WNS as a potential material to be employed for the uptake of pollutants. Removal of pollutants in column was reliant on the bed height, initial pollutants concentration and the flowing time.

The uptake process revealed to be enhanced at lesser influent pollutants concentration, lesser flowing rate and enhanced bed height. The modification of WNS with the surfactant rendered the charge present on adsorbent surface positive, which improved the uptake of CR and BPA in the fixed column bed. The breakthrough curve was successfully predicted by Yan model, demonstrating that it was very appropriate for WNS-CTAB column design. Moreover, the adsorbent exhibited reusability potential for the uptake of pollutants from solution. This will guarantee a sustainable way of removing CR and BPA from polluted water.

**Authors' contribution**

1). Evans Dovi (evansdovy@gmail.com): Conceptualization; Methodology; Formal analysis; Investigation; Writing original draft; Visualization.

2). Aaron Albert Aryee (a.niiayi@yahoo.com): Software, writing-review and editing, formal analysis

3). Alexander Nti Kani (mykani@yahoo.com): Writing-review and editing, formal analysis

4). Farid Mzee Mpatani (papilampatani@gmail.com): Software, formal analysis, Writing-review and editing.

5). Jianjun Li (lijianjun@zzu.edu.cn) Visualization; Supervision; funding acquisition

6). Lingbo Qu (qulingbo@zzu.edu.cn): Resources, funding acquisition.

7). Zhaohui Li (zhaohui.li@zzu.edu.cn): Visualization; Supervision; funding acquisition.

8). Runping Han (rphan67@zzu.edu.cn): Conceptualization; Resources; Project administration; Writing-review and editing, Visualization; Supervision; Funding acquisition

**Funding**

This work was supported in part by the National Natural Science Foundation of China (21205108, 21974125), the Foundation for University Key Teacher by Henan Province (2017GGJS007), and the Key Scientific Research Project in Universities of Henan Province (19A150048).

**Availability of data and material**

The dataset generated and analysed during this study could be obtained from the corresponding author on reasonable request

**Declaration of interests**

The authors declare that they have no known competing financial interests or personal relationships that could have appeared to influence the work reported in this paper

**Ethics approval**

Not Applicable

**Consent to participate**

Not Applicable

**Consent for publication**

Not Applicable

**References**

Aguayo-villarreal IA, Bonilla-petriciolet A, Hernández-montoya V, Montes-morán MA, Reynel-avila HE, (2011) Batch and column studies of $Zn^{2+}$ removal from aqueous solution using chicken feathers as sorbents. Chem. Eng. J., 167(1), 67–76. https://doi.org/10.1016/j.cej.2010.11.107

Ahmad AA, Hameed BH, (2010) Fixed-bed adsorption of reactive azo dye onto granular activated carbon prepared from waste.J. Hazard. Mater. 175, 298–303. https://doi.org/10.1016/j.jhazmat.2009.10.003

Aksu Z, Gonen F, (2004) Biosorption of phenol by immobized activated sludge in a continuous packed bed: prediction of breakthrough curves. Process Biochem. 39, 599–613. http://doi.org/10.1016/S0032-9592(03)00132-8

Aryee AA, Mpatani FM, Kani AN, Dovi E, Han R.P, Li ZH, Qu LB, (2020a) Iminodiacetic acid functionalized magnetic peanut husk for the removal of methylene blue from solution: characterization and equilibrium studies. Environ. Sci. Pollut. Res. 27, 40316–40330. https://doi.org/10.1007/s11356-020-10087-6

Aryee AA, Mpatani FM, Zhang X, Kani AN, Dovi E, Han RP, Li ZH, Qu LB, (2020b) Iron (III) and iminodiacetic acid functionalized magnetic peanut husk for the removal of phosphate from solution: Characterization, kinetic and equilibrium studies. J. Clean. Prod. 268, 122191. https://doi.org/10.1016/j.jclepro.2020.122191

Aryee AA, Mpatani FM, Du YY, Kani AN, Dovi E, Han RP, Li ZH, Qu. LB (2021) $Fe_3O_4$ and Iminodiacetic acid modified peanut husk as a novel adsorbent for the uptake of Cu (II) and Pb (II) in aqueous solution: Characterization, equilibrium and kinetic study. Environ. Pollut. 268, 115729. https://doi.org/10.1016/j.envpol.2020.115729

Auta M, Hameed BH, (2014) Chitosan – clay composite as highly effective and low-cost adsorbent for batch and fixed-bed adsorption of methylene blue. Chem. Eng. J. 237, 352–361. https://doi.org/10.1016/j.cej.2013.09.066

Banerjee M, Kumar R, Kumar S, (2018) Cr(VI) adsorption by a green adsorbent walnut shell : Adsorption studies , regeneration studies , scale-up design and economic feasibility. Process Saf. Environ. 116, 693–702. https://doi.org/10.1016/j.psep.2018.03.037

Baral SS, Das N, Ramulu TS, Sahoo SK, Das SN, Chaudhury GR, (2009) Removal of Cr(VI ) by thermally activated weed Salvinia cucullata in a fixed-bed column. J. Hazard. Mater. 161, 1427–1435. https://doi.org/10.1016/j.jhazmat.2008.04.127

Bhaumik M, McCrindle R, Maity A, (2013) Efficient removal of Congo red from aqueous solutions by adsorption onto interconnected polypyrrole-polyaniline nanofibres. Chem. Eng. J., 228, 506–515. https://doi.org/10.1016/j.cej.2013.05.026

Calero M, Hernáinz F, Blázquez G, Tenorio G, (2009) Study of Cr(III) biosorption in a fixed-bed column. J. Hazard. Mater. 171, 886–893. https://doi.org/10.1016/j.jhazmat.2009.06.082

Cao JS, Lin JX, Fang F, Zhang MT, Hu ZR, (2014) A new absorbent by modifying walnut shell for the removal of anionic dye: Kinetic and thermodynamic studies. Bioresour. Technol. 163, 199–205. https://doi.org/10.1016/j.biortech.2014.04.046

Chang KL, Hsieh JF, Ou BM, Chang MH, Hseih WY, Lin JH, Chen ST, (2012) Adsorption Studies on the Removal of an Endocrine-Disrupting Compound (Bisphenol A) using Activated Carbon from Rice Straw Agricultural Waste. Sep. Sci. Technol. 47(10), 1514–1521. https://doi.org/10.1080/01496395.2011.647212

Chen S, Yue Q, Gao B, Li Q, Xu X, Fu K (2012) Adsorption of hexavalent chromium from aqueous solution

by modified corn stalk : A fixed-bed column study. Bioresour. Technol. 113, 114–120. https://doi.org/10.1016/j.biortech.2011.11.110

Clark RM, (1987) Evaluating the cost and performance of field-scale granular activated carbon systems. Environ. Sci. Technol. 21, 573–580. https://doi.org/10.1021/es00160a008

Dovi E, Kani AN, Aryee A A, Ma J, Li JJ, Li ZH, Qu LB, Han RP (2021) Decontamination of Bisphenol A and Congo red dye from Solution by using CTAB functionalized walnut shell. Environ.Sci. Pollut. Res. in press. https://doi.org/10.1007/s11356-021-12550-4

Han RP, Wang Y, Sun Q, Wang LL, Song JY, He XT, Dou CC (2010) Malachite green adsorption onto natural zeolite and reuse by microwave irradiation. J Hazard Mater 175(1-3), 1056–1061. https://doi.org/10.1016/j.jhazmat.2009.10.118

Han RP, Wang Y, Zhao X, Wang YF, Xie FL, Cheng JM, Tang MS (2009) Adsorption of methylene blue by phoenix tree leaf powder in a fixed-bed column : experiments and prediction of breakthrough curves. Desalination 245(1–3), 284–297. https://doi.org/10.1016/j.desal.2008.07.013

Hou H, Zhou R, Wu P, Wu L (2012) Removal of Congo red dye from aqueous solution with hydroxyapatite/chitosan composite. Chem. Eng. J., 211–212, 336–342. https://doi.org/10.1016/j.cej.2012.09.100

Kani AN, Dovi E, Mpatani FM, Li ZH, Han RP, Qu LB (2020) Tiger nut residue as a renewable adsorbent for methylene blue removal from solution : adsorption kinetics , isotherm , and thermodynamic studies. Desalin. Water Treat. 191, 426–437. https://doi.org/10.5004/dwt.2020.25735

Kani AN, Dovi E, Aryee AA, Mpatani, FM, Han, RP, Li ZH, Qu LB 2021. Polyethyleneimine modified Tiger nut residue for removal of Congo red from solution Desalin. Water Treat. in press. https://doi.org/10.5004/dwt.2021.26765.

Kumar PS, Ramalingam S, Senthamarai C, Niranjanaa M, Vijayalakshmi P, Sivanesan S (2010) Adsorption of dye from aqueous solution by cashew nut shell : Studies on equilibrium isotherm , kinetics and thermodynamics of interactions. Desalination 261(1-2), 52–60. https://doi.org/10.1016/j.desal.2010.05.032

Kundu S, Simon S, Pal A, Kumar S, Mandal M, Pal T (2004) Removal of arsenic using hardened paste of Portland cement : batch adsorption and column study. J. Water Res. 38, 3780–3790. https://doi.org/10.1016/j.watres.2004.06.018

Li JY, Ma J, Guo QH, Zhang SL, Han HY, Zhang SS, Han RP (2020) Adsorption of hexavalent chromium from solution using modified walnut shell. Water Sci.Technol. 81(4), 824–833. https://doi.org/10.2166/wst.2020.165

Mane VS, Vijay Babu PV (2013) Kinetic and equilibrium studies on the removal of Congo red from aqueous solution using Eucalyptus wood (Eucalyptus globulus) saw dust. J. Taiwan Inst. Chem. E .44(1), 81–88. https://doi.org/10.1016/j.jtice.2012.09.013

Mpatani FM, Aryee AA, Kani AN, Guo Q, Dovi E, Qu LB, Han RP (2020 a) Uptake of micropollutant-bisphenol A , methylene blue and neutral red onto a novel bagasse- b -cyclodextrin polymer by adsorption process. Chemosphere 259, 127439. https://doi.org/10.1016/j.chemosphere.2020.127439

Mpatani FM, Aryee AA, Kani AN, Wen K, Dovi E, Qu LB, Li ZH, Han RP (2020b) Removal of methylene blue from aqueous medium by citrate modified bagasse: kinetic, equilibrium and thermodynamic study. Bioresour. Technol. Rep. 11, 100463. https://doi.org/10.1016/j.biteb.2020.100463

Olgun A, Atar N, Wang S (2013) Batch and column studies of phosphate and nitrate adsorption on waste solids containing boron impurity. Chem. Eng. J. 222, 108–119. https://doi.org/10.1016/j.cej.2013.02.029

Paterni I, Granchi C, Minutolo F (2018) Risks and benefits related to alimentary exposure to xenoestrogens. Critical Rev. Food Sci. Nutr. 57(16), 3384–3404. https://doi.org/10.1080/10408398.2015.1126547

Shang Y, Zhang J, Wang X, Zhang R, Xiao W, Zhang S (2015) Use of polyethyleneimine-modified wheat straw for adsorption of Congo red from solution in batch mode. Desalin. Water Treat. 57(19), 8872–8883. https://doi.org/10.1080/19443994.2015.1027280

Vinodhini V, Das N (2010) Packed bed column studies on Cr ( VI ) removal from tannery wastewater by neem sawdust. Desalination 264(1-2), 9–14. https://doi.org/10.1016/j.desal.2010.06.073

Xia C, Jing Y, Jia Y, Yue D, Ma J, Yin X (2011) Adsorption properties of congo red from aqueous solution on modified hectorite: Kinetic and thermodynamic studies. Desalination 265(1–3), 81–87. https://doi.org/10.1016/j.desal.2010.07.035

Xu X, Gao BY, Jin, B, Yue QY (2016) Removal of anionic pollutants from liquids by biomass materials: A review. J. Mol. Liq. 215, 565–595. http://dx.doi.org/10.1016/j.molliq.2015.12.101

Yan G, Viraraghavan T, Chen M (2001) A new model for heavy metal removal in a biosorption column, Adsorpt. Sci. Technol. 19, 25–43. https://doi.org/10.1260/0263617011493953

Zhang W, Li H, Kan X, Dong L, Yan H, Jiang Z, Cheng R (2012) Adsorption of anionic dyes from aqueous solutions using chemically modified straw. Bioresour Technol, 117, 40–47. https://doi.org/10.1016/j.biortech.2012.04.064

Zhang RD, Zhang JH, Zhang XN, Dou CC, Han RP ( 2014) Adsorption of congo red from aqueous solutions using cationic surfactant modified wheat straw in batch mode: Kinetic and equilibrium study. J. Taiwan Inst. Chem. E. 45, 2578–2583. https://doi.org/10.1016/j.jtice.2014.06.009

Zhao H, Yu Q, Li M, Sun S ( 2020) Preparation and water vapor adsorption of “green” walnut-shell activated carbon by $CO_2$ physical activation. Ads. Sci. Technol. 38(1-2), 60–76. https://doi.org/10.1177/0263617419900849

Zhou T, Lu W, Liu L, Zhu H, Jiao Y, Zhang S, Han R (2015) Effective adsorption of light green anionic dye from solution by CPB modi fi ed peanut in column mode. J. Mol. Liq., 211, 909–914. https://doi.org/10.1016/j.molliq.2015.08.018

Zhou Y, Lu P, Lu J (2012) Application of natural biosorbent and modified peat for bisphenol A removal from aqueous solutions. Carbohyd. Polym. 88(2), 502–508. https://doi.org/10.1016/j.carbpol.2011.12.034

**Captions of figures**

Fig. 1 Comparison of breakthrough curves for WNS and WNS-CTAB for adsorption of CR (a) and BPA (b) ($Z$= 6 cm, $C_0$ =50 mg $L^{-1}$, $v$ = 10 mL $min^{-1}$).

Fig. 2 Breakthrough curves of CR (a) and BPA (b) adsorption onto WNS-CTAB at various flow rates ($C_0$ = 50 mg $L^{-1}$, $Z$= 6 cm).

Fig. 3 Breakthrough curves of CR (a) and BPA (b) adsorption onto WNS-CTAB at various concentration ($v$ = 10 mL $min^{-1}$, $Z$= 6 cm).

Fig. 4 Breakthrough curves of CR (a) and BPA (b) adsorption onto WNS-CTAB at various bed heights ($C_0$ = 50 mg $L^{-1}$, $v$ = 10 mL $min^{-1}$).

Fig. 5 Column desorption curve and recycle curve for CR (a, b) and BPA (c, d), respectively.

**Captions of Tables**

**Table 1a** Parameters in fixed-bed column for CR and BPA adsorption by WNS-CTAB

**Table 1b** Thomas model parameters for CR and BPA adsorption at different operating conditions

**Table 2** Clark model parameters for CR and BPA uptake at various conditions

**Table 3** Yan model parameters for CR and BPA adsorption at different conditions

**Table 4** Adsorption and elution process parameters for adsorption–desorption cycles

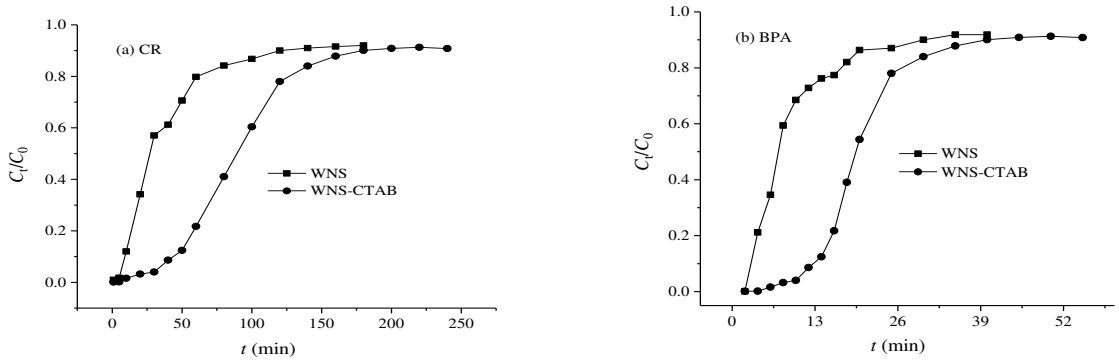


Fig. 1 Comparison of breakthrough curves for WNS and WNS-CTAB for adsorption of CR (a) and BPA (b) ($Z$= 6 cm, $C_0$ =50 mg $L^{-1}$, $v$ = 10 mL $min^{-1}$).

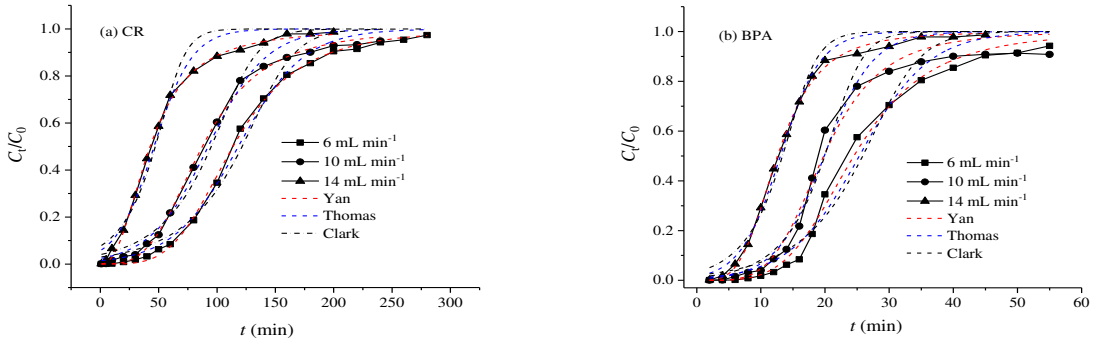


Fig. 2. Breakthrough curves of CR (a) and BPA (b) adsorption onto WNS-CTAB at various flow rates ($C_0$ = 50 mg $L^{-1}$, $Z$= 6 cm).

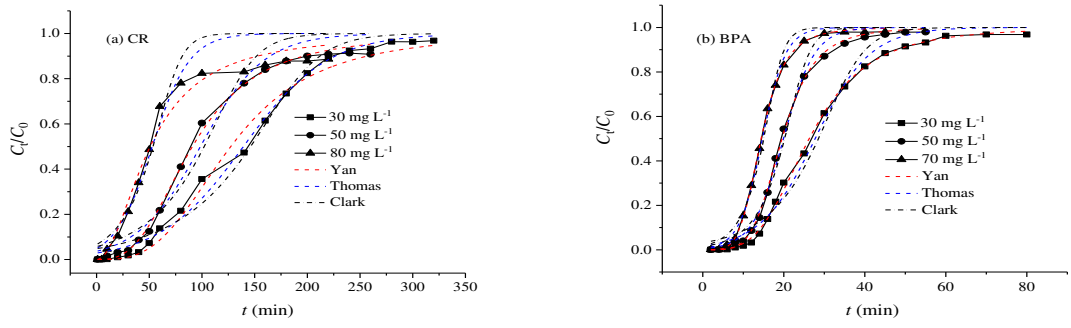


Fig. 3. Breakthrough curves of CR (a) and BPA (b) adsorption onto WNS-CTAB at various concentration ($v$ = 10 mL $min^{-1}$, $Z$= 6 cm).

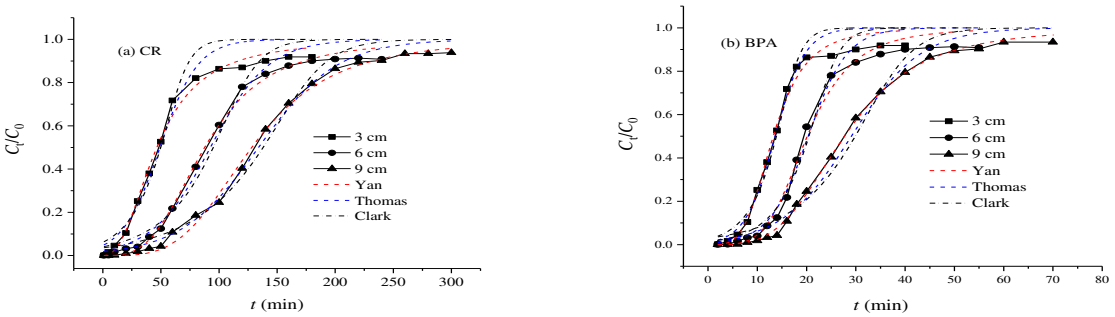


Fig. 4. Breakthrough curves of CR (a) and BPA (b) adsorption onto WNS-CTAB at various bed heights ($C_0$ = 50 mg $L^{-1}$, $v$ = 10 mL $min^{-1}$).

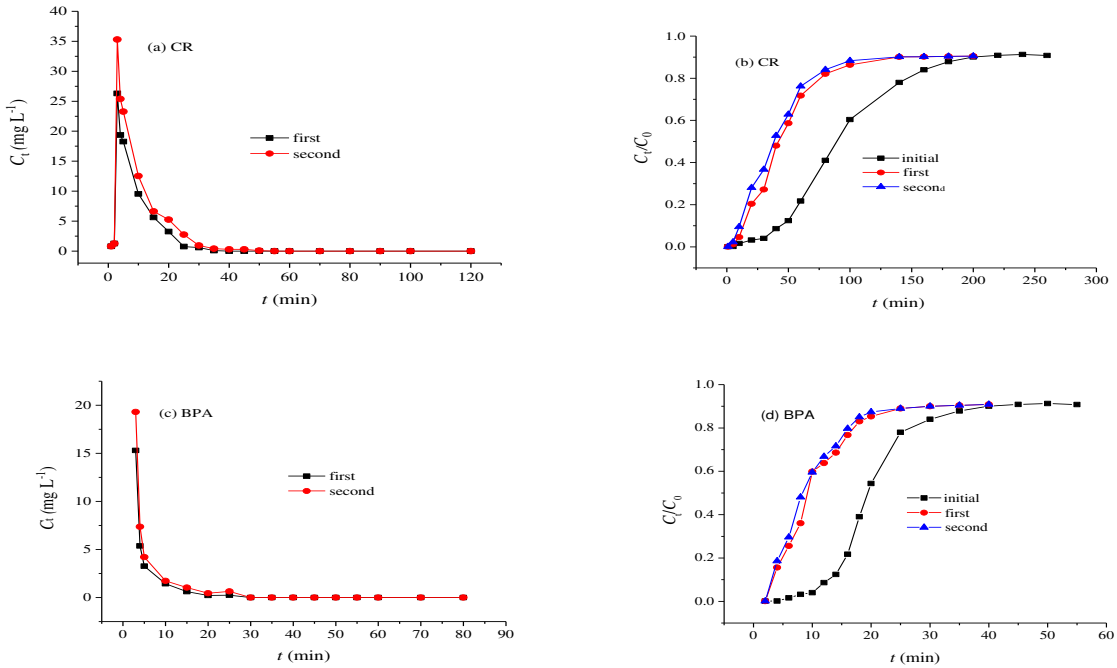


Fig. 5. Column desorption curve and recycle curve for CR (a, b) and BPA (c, d), respectively.

Table 1a. Parameters in fixed-bed column for CR and BPA uptake by WNS-CTAB

| | | | CR | | BPA | |
|---|---|---|---|---|---|---|
| $C_o$ (mg $L^{-1}$) | $v$ (mL $min^{-1}$) | $Z$(cm) | $q_{total}$ | $q_{exp}$ (mg $g^{-1}$) | $q_{total}$ | $q_{exp}$ (mg $g^{-1}$) |
| 30 | 10 | 6 | 42.2 | 13.0 | 8.86 | 2.73 |
| 50 | 10 | 6 | 43.1 | 13.3 | 10.6 | 3.27 |
| 80 | 10 | 6 | 57.3 | 17.6 | | |
| 70 | 10 | 6 | | | 10.9 | 3.36 |
| 50 | 6 | 6 | 37.2 | 11.4 | 8.06 | 2.48 |
| 50 | 14 | 6 | 37.7 | 11.6 | 9.95 | 3.06 |
| 50 | 10 | 3 | 19.8 | 12.1 | 5.26 | 3.20 |
| 50 | 10 | 9 | 69.5 | 14.2 | 15.1 | 3.10 |

Table 1b. Thomas model parameters for CR and BPA adsorption at different operating conditions

| $C_o$ (mg $L^{-1}$) | $V$ (mL $min^{-1}$) | $Z$ (cm) | $k_{Th}$ (mL $mg^{-1}$ $min^{-1}$) | $q_{e(exp)}$ (mg $g^{-1}$) | $q_o$ (mg $g^{-1}$) | $R^2$ | SSE |
|---|---|---|---|---|---|---|---|
| **CR** | | | | | | | |
| 30 | 10 | 6 | 0.840 ± 0.04 | 13.0 | 12.9 ± 0.23 | 0.993 | 0.020 |
| 80 | 10 | 6 | 0.704 ± 0.13 | 17.6 | 13.0 ± 0.87 | 0.932 | 0.117 |
| 50 | 6 | 6 | 0.715 ± 0.04 | 11.5 | 11.0 ± 0.18 | 0.993 | 0.020 |
| 50 | 10 | 6 | 0.806 ± 0.06 | 15.2 | 14.2 ± 0.34 | 0.989 | 0.026 |
| 50 | 14 | 6 | 1.22 ± 0.12 | 11.6 | 9.94 ± 0.36 | 0.983 | 0.033 |
| 50 | 10 | 3 | 1.23 ± 0.17 | 12.1 | 15.0 ± 0.73 | 0.966 | 0.059 |
| 50 | 10 | 9 | 0.593 ± 0.03 | 14.2 | 13.7 ± 0.21 | 0.993 | 0.019 |
| **BPA** | | | | | | | |
| 30 | 10 | 6 | 4.91± 0.30 | 2.73 | 2.56 ± 0.05 | 0.990 | 0.024 |
| 70 | 10 | 6 | 4.97 ± 0.29 | 3.36 | 3.18 ± 0.03 | 0.996 | 0.008 |
| 50 | 6 | 6 | 3.68 ± 0.36 | 2.48 | 3.90 ± 0.10 | 0.978 | 0.049 |
| 50 | 10 | 6 | 5.31 ± 0.73 | 2.72 | 3.06 ± 0.09 | 0.971 | 0.070 |
| 50 | 14 | 6 | 6.39 ± 0.38 | 3.06 | 2.81 ± 0.04 | 0.992 | 0.001 |
| 50 | 10 | 3 | 6.62 ± 0.71 | 3.20 | 4.15 ± 0.11 | 0.977 | 0.039 |
| 50 | 10 | 9 | 2.85 ± 0.20 | 3.10 | 2.98 ± 0.07 | 0.986 | 0.037 |

Table 2. Clark model parameters for CR and BPA uptake at various conditions

| $C_o$ (mg $L^{-1}$) | $V$ (mL $min^{-1}$) | $Z$ (cm) | $A$ | $r$ | $n$ | $R^2$ | SSE |
|---|---|---|---|---|---|---|---|
| **CR** | | | | | | | |
| 30 | 10 | 6 | 2112 ± 1039 | 0.0417 ± 0.0031 | 3.52 | 0.986 | 0.0422 |
| 50 | 10 | 6 | 1353 ± 1068 | 0.0554 ± 0.0079 | 3.52 | 0.958 | 0.0986 |
| 80 | 10 | 6 | 931 ± 1091 | 0.0987 ± 0.022 | 3.52 | 0.913 | 0.150 |
| 50 | 6 | 6 | 7135 ± 5299 | 0.0602 ± 0.0059 | 3.52 | 0.982 | 0.0515 |
| 50 | 14 | 6 | 661 ± 476 | 0.105 ± 0.015 | 3.52 | 0.968 | 0.0614 |
| 50 | 10 | 3 | 1165 ± 1173 | 0.111 ± 0.020 | 3.52 | 0.950 | 0.0858 |
| 50 | 10 | 9 | 4525 ± 2792 | 0.0497 ± 0.0043 | 3.52 | 0.983 | 0.0498 |
| **BPA** | | | | | | | |
| 30 | 10 | 6 | 2533 ± 1553 | 0.228 ± 0.021 | 3.26 | 0.980 | 0.061 |
| 50 | 10 | 6 | 14175 ± 11294 | 0.407 ± 0.041 | 3.26 | 0.987 | 0.035 |
| 70 | 10 | 6 | 9783 ± 6636 | 0.522 ± 0.044 | 3.26 | 0.989 | 0.023 |
| 50 | 6 | 6 | 6756 ± 6714 | 0.289 ± 0.039 | 3.26 | 0.963 | 0.084 |
| 50 | 14 | 6 | 2173 ± 1324 | 0.475 ± 0.044 | 3.26 | 0.985 | 0.027 |
| 50 | 10 | 3 | 4234 ± 4041 | 0.505 ± 0.067 | 3.26 | 0.968 | 0.059 |
| 50 | 10 | 9 | 2878 ± 2015 | 0.222 ± 0.0023 | 3.26 | 0.972 | 0.077 |

Table 3. Yan model parameters for CR and BPA adsorption at different conditions

| $C_0$ (mg $L^{-1}$) | $v$ (mL $min^{-1}$) | $Z$ (cm) | $a$ | $b$ (mL) | $q_o$ (mg $g^{-1}$) | $R^2$ | SSE |
|---|---|---|---|---|---|---|---|
| **CR** | | | | | | | |
| 30 | 10 | 6 | 3.13 ± 0.19 | 1273 ± 32 | 11.8 | 0.991 | 0.027 |
| 50 | 10 | 6 | 2.86 ± 0.09 | 909.7± 12.9 | 14.0 | 0.997 | 0.006 |
| 80 | 10 | 6 | 2.00 ± 0.18 | 509.0 ± 23.5 | 12.5 | 0.980 | 0.035 |
| 50 | 6 | 6 | 3.95 ± 0.10 | 682.4 ± 5.1 | 10.5 | 0.999 | 0.004 |
| 50 | 14 | 6 | 2.41 ± 0.07 | 597.9 ± 7.5 | 9.20 | 0.998 | 0.003 |
| 50 | 10 | 3 | 2.39 ± 0.15 | 465.1 ± 12.7 | 14.2 | 0.992 | 0.013 |
| 50 | 10 | 9 | 3.69 ± 0.14 | 1281 ± 15 | 13.1 | 0.997 | 0.009 |
| **BPA** | | | | | | | |
| 30 | 10 | 6 | 3.65 ± 0.07 | 263.0± 1.8 | 2.43 | 0.999 | 0.0031 |
| 50 | 10 | 6 | 4.83 ± 0.13 | 196.7 ± 1.2 | 3.01 | 0.999 | 0.0030 |
| 70 | 10 | 6 | 4.84 ± 0.07 | 144.2 ± 0.5 | 3.11 | 0.999 | 0.0009 |
| 50 | 6 | 6 | 4.18 ± 0.21 | 147.0 ± 2.2 | 2.26 | 0.994 | 0.0142 |
| 50 | 14 | 6 | 3.87 ± 0.11 | 176.3 ± 1.4 | 2.71 | 0.998 | 0.0030 |
| 50 | 10 | 3 | 3.96 ± 0.32 | 132.5 ± 2.8 | 4.04 | 0.987 | 0.0217 |
| 50 | 10 | 9 | 3.65 ± 0.08 | 276.8 ± 2.1 | 2.80 | 0.999 | 0.0038 |

Table 4. Adsorption and elution process parameters for adsorption–desorption cycles

| | CR | | | | BPA | | | |
|---|---|---|---|---|---|---|---|---|
| Cycle | $q_e$ (mg $g^{-1}$) | $t_b$ (min) at $C_t/C_0$= 0.1 | $R$ % | Desorption efficiency | $q_e$ (mg $g^{-1}$) | $t_b$ (min) at $C_t/C_0$= 0.1 | $R$ % | Desorption efficiency |
| Initial | 13.3 | 42 | 41.2 | | 3.27 | 13 | 38.6 | |
| First | 8.47 | 13 | 34.4 | 77.9 | 1.88 | 3 | 34.9 | 42.7 |
| Second | 5.90 | 8 | 29.5 | 71.2 | 1.09 | 3 | 27.2 | 58.8 |

## Highlights

- Walnut shell was successfully modified with CTAB (WNS-CTAB)
- Continuous column uptake quantity of WNS was enhanced after modification
- Breakthrough curves were better described by Yan kinetic model
- WNS-CTAB can to be regenerated and reused for adsorption

## Graphical Abstract

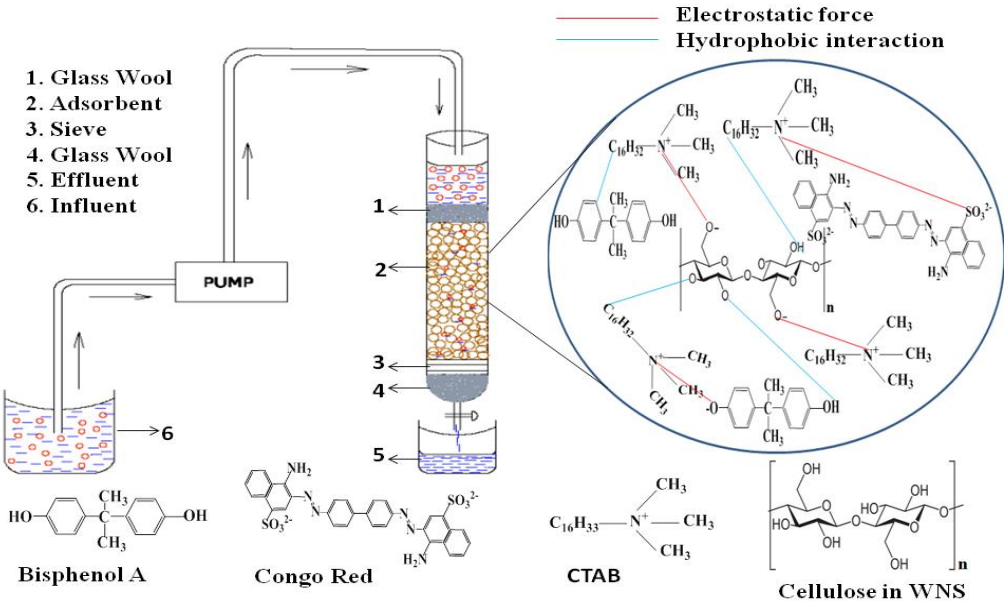

# Figures

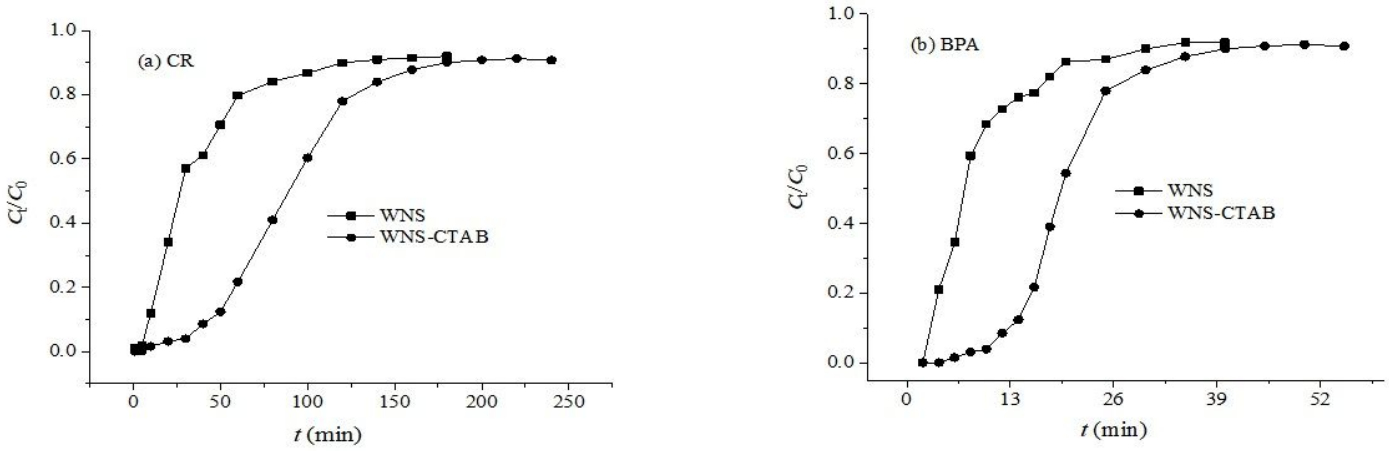


**Figure 1**

Comparison of breakthrough curves for WNS and WNS-CTAB for adsorption of CR (a) and BPA (b) (Z= 6 cm, C0 =50 mg L−1, v = 10 mL min−1).

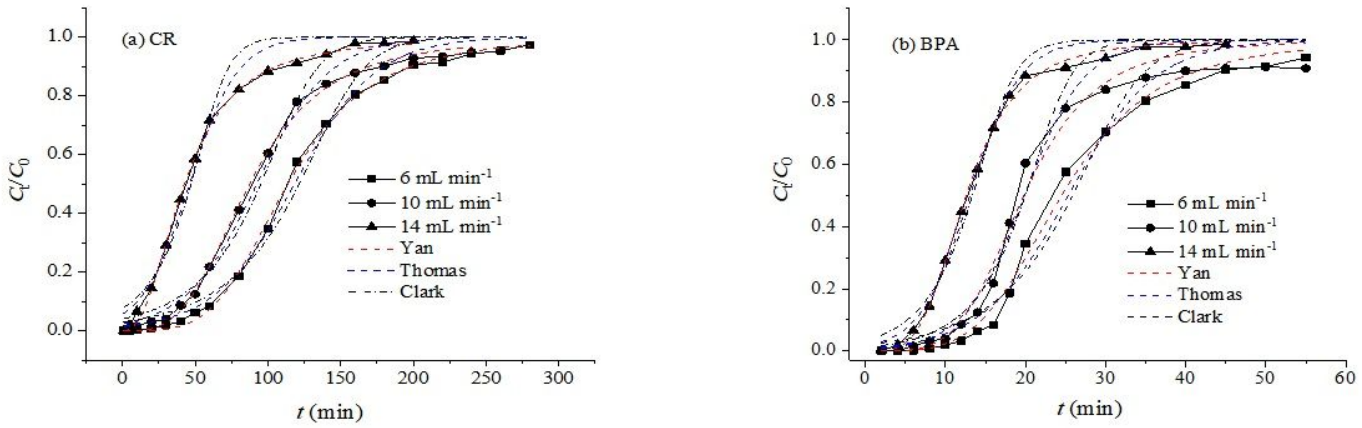


**Figure 2**

Breakthrough curves of CR (a) and BPA (b) adsorption onto WNS-CTAB at various flow rates (C0 = 50 mg L−1, Z= 6 cm).

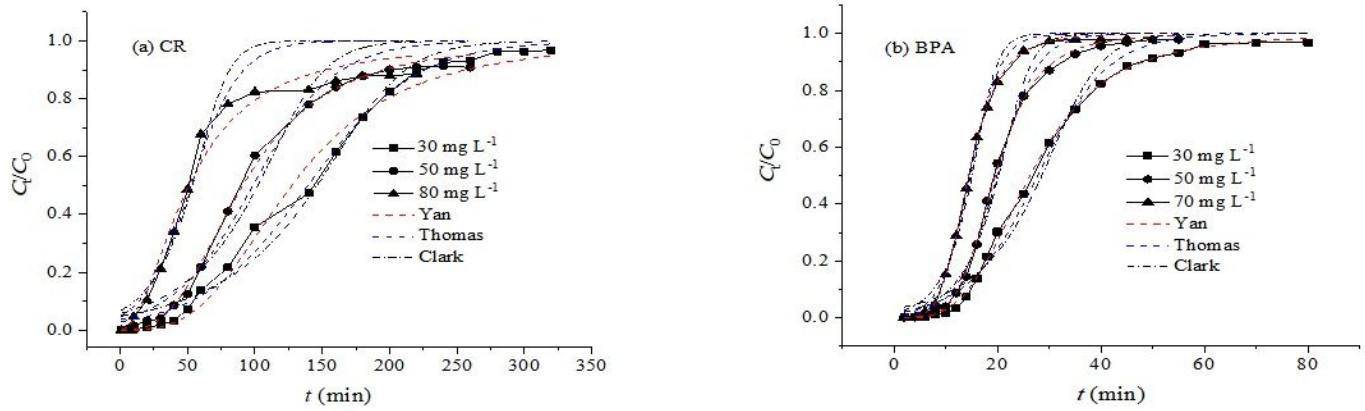


## Figure 3

Breakthrough curves of CR (a) and BPA (b) adsorption onto WNS-CTAB at various concentration (v = 10 mL min−1, Z= 6 cm).

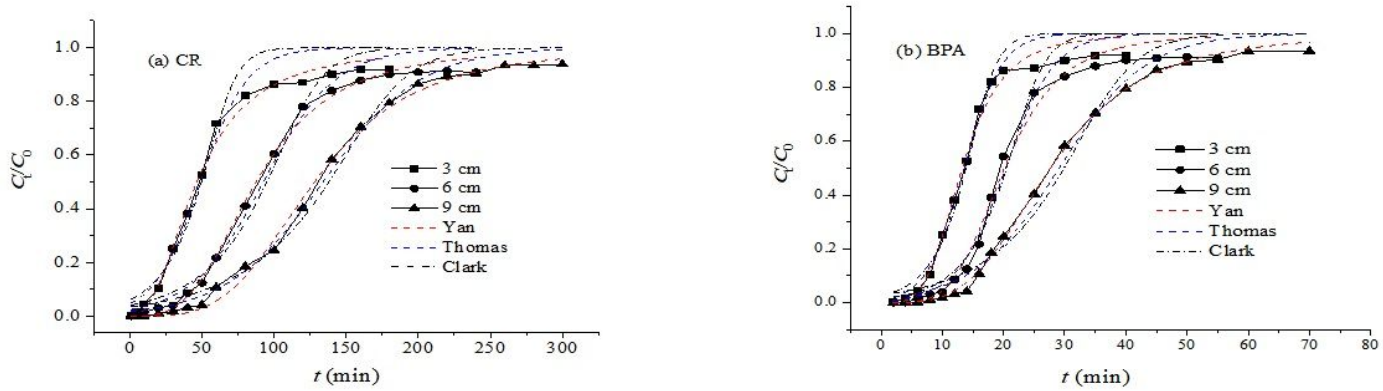


## Figure 4

Breakthrough curves of CR (a) and BPA (b) adsorption onto WNS-CTAB at various bed heights (C0 = 50 mg L−1, v = 10 mL min−1).

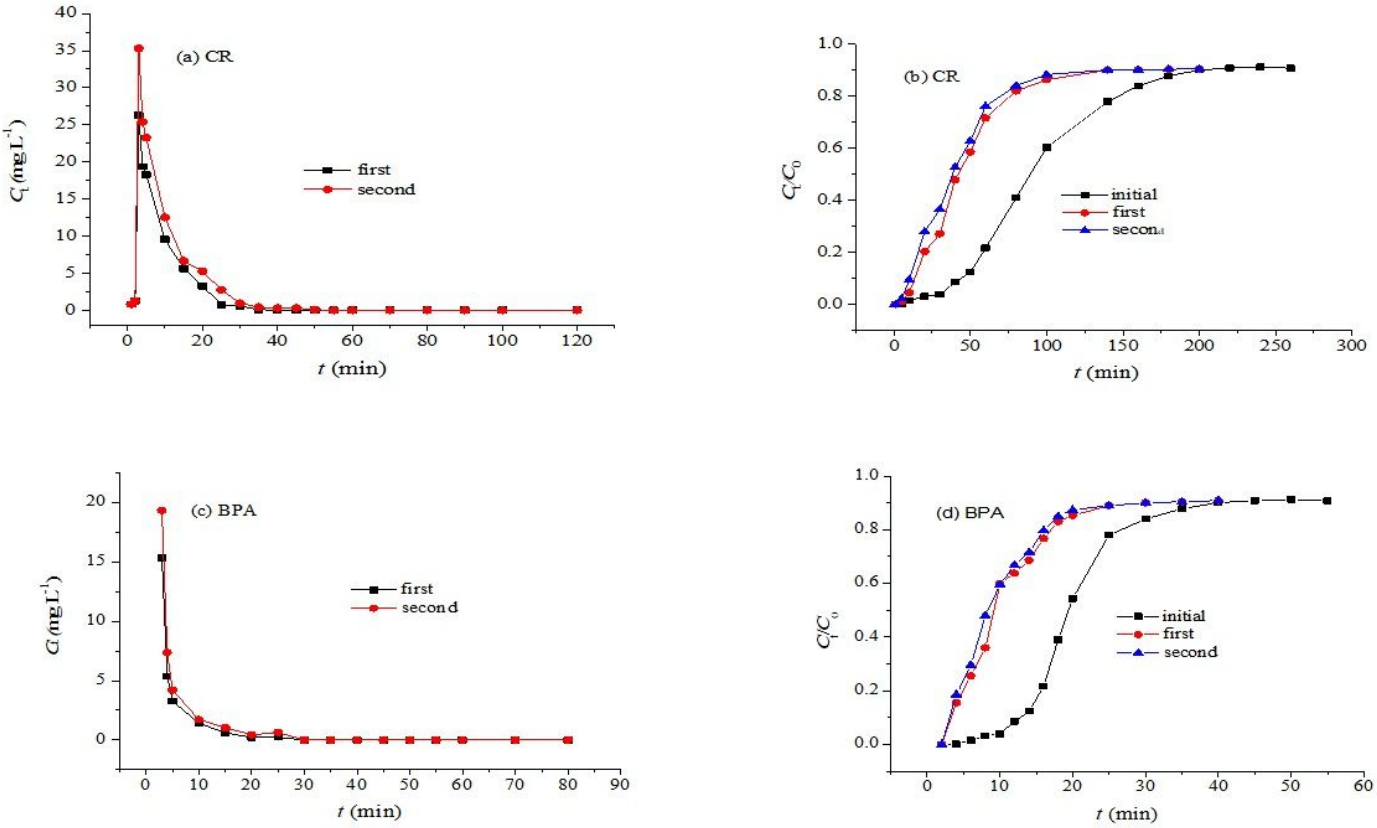


**Figure 5**

Column desorption curve and recycle curve for CR (a, b) and BPA (c, d), respectively.

# Supplementary Files

This is a list of supplementary files associated with this preprint. Click to download.

- GraphicalAbstract.jpg